

Developing and Modeling a plane 3 DOF Compliant Micromanipulator by means of a dedicated MBS code

Balucani, M. *, Belfiore, N. P. **, Crescenzi, R. *, Genua, M. *, Verotti, M. **

*Dept. Information Engineering, Electronic and Telecommunications, balucani@die.uniroma1.it

**Dept. Mechanical and Aerospace Engineering, belfiore@dma.ing.uniroma1.it
Sapienza University of Rome, via Eudossiana, 18 – 00184 Rome, Italy

ABSTRACT

In the present investigation, a new Multi-Body System code has been introduced for studying the static and dynamic analysis of micro-compliant mechanisms. Since the first natural frequency of elastic microsystems can be expected to be quite high, the integration time was significantly reduced and the step time interval was also reduced during integration. The code applies the Lagrange Multiplier method of dynamic analysis to the pseudo-rigid body model of the compliant microsystem, the latter being obtained by imposing the centers of the revolute joints of the model be coincident with the centers of the elastic weights of the flexural arcs of the real system. The actual construction of one-to-one scaled prototypes have been also described as a first step to a possible future comparison of the code results and the MEMS real behaviour. For this reason, two adopted construction techniques have been described: copper electro deposition and RIE on silicon

Keywords: Multibody, MEMS, Compliant Mechanisms, RIE, microrobots.

1 INTRODUCTION

During the last two years, our research team, has been developing a new family of MEMS (Micro Electro Mechanical System) based on selective compliant. Several different technologies have been investigated and tested, up to now, in order to enlarge the workspace of the micromanipulator end effector without affecting its functional capability. Unfortunately, such a task is not easy because in compliant mechanisms, a large workspace implies large deformations and so it is very likely to overpass the material elasticity region. The construction techniques have been involving a variety of methods, and, in particular, surface and bulk micromachining.

A fundamental task for the development of this family of MEMS is the simulation, which allows to optimize the experimental activities by selecting the most feasible structures. This part of the investigation relies on a proper model of the system and, of course, on an efficient tool which is able to evaluate the model evolution as a response of the external applied action. This allows to predict the structure stress and deflection in dynamic conditions.

In the present paper, some 3 D.O.F. (degrees of freedom) compliant micro robots will be firstly presented. Then, the corresponding pseudo-rigid-body will be obtained together

with its dynamic model. The latter will be simulated by means of the classical techniques of the Dynamic Simulation of Multi Body Systems. Finally, some details concerning the actual construction of the real MEMS will be presented.

2 THE 3 DOF COMPLIANT MICROMANIPULATOR

An alternative solution to the traditional compliant mechanisms has been proposed in [1], where a new flexural hinge has been introduced. A basic principle is therein adopted to introduce equivalent revolute pairs into a compliant mechanisms, namely, that compliance provides (limited) mobility, while geometry provides accuracy. The new idea is based both on the selective compliance of sub-parts with smaller sections (flexible joints), and on the actions of classic conjugate surfaces (kinematic elements). According to the patent [1], the center W of the conjugate profiles in the motion plane is coincident with the center of the elastic weights of the flexural thin part.

Using this compliant hinge, several structures can be conceived, such as, for example, the parallel structure depicted in Figure 1 *a*), which will be the focus of the present research. Thanks to the compliant hinges embedded into such structure, the top platform 4 has 3 D.O.F with respect to the base link 1. This platform can be actuated in several ways, for example by means of electrostatic comb drives or by means or remotely actuated tendons.

3 THE DEVELOPED CODE FOR THE DYNAMIC SIMULATION OF THE 3 DOF COMPLIANT MICROMANIPULATOR

From the compliant plane structure represented in Figure 1 *a*) it is possible to obtain a so-called equivalent pseudo-rigid body mechanism by considering the largest sub-parts as rigid links (AB, BC, CD, DE, EF, FA), and the thinnest ones as flexible sub-parts, and by substituting the latter with a classical revolute joints having their centers in A, B, C, D, E, or F, respectively (such points being coincident with the centers W , as above defined, of the elastic weights). Hence, the pseudo-rigid body equivalent mechanism is the six bar linkage ABCDEF.

Within reasonable tolerances, the pseudo-rigid body equivalent six bar linkage behaves like the original mechanism, the former being much more difficult to simulate. Furthermore, the effect of the joint elasticity and friction can

be simulated by adding one revolte spring and one revolte damper for each kinematic pair.

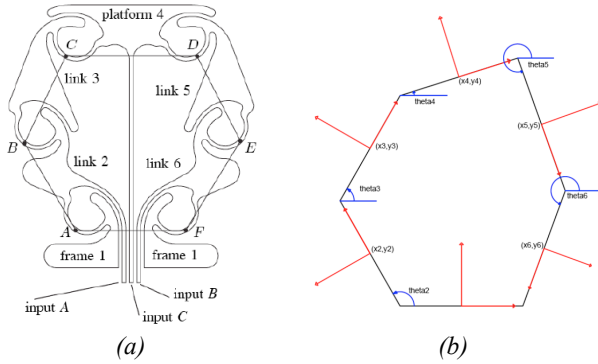


Figure 1: Geometry and its corresponding pseudo-rigid equivalent mechanism and the Ref. Point Coordinates.

3.1 Definition of the set of coordinates

By adopting the Reference Point Coordinates, 3 coordinates can be introduced for each mobile body, which defines a $n = 15$ coordinates vector $\{q\}$, the latter satisfying $m = 12$ constraint equations

$$\{\Psi(q,t)\} = \{0\}, \tag{1}$$

where $\{\Psi(q,t)\}$ is the constraint vector. While the constraint equations are independent, the system has $F = n - m = 3$ degrees of freedom (D.O.F.). Therefore, for the present case there will be $F = 3$ independent coordinates $\{v\}$ and $m = 12$ dependent coordinates $\{u\}$.

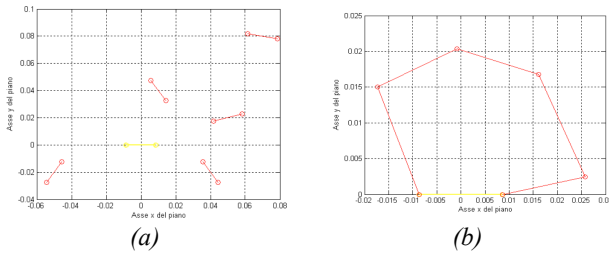


Figure 2. Position of the links in the motion plane at the beginning (a) and at the end (b) of the iterative process.

3.2 Assembly problem and kinematic analysis

The assembly problem consists in the identification of all the dependent coordinates $\{u\}$ which satisfy equation (1) for a given set of independent coordinates $\{v\}$. This problem has been easily solved numerically by applying the Newton-Raphson algorithm to solve the non-linear system of 12 equations (1) with respect to the 12 variables $\{u\}$. An

example of the graphical output of the program is given in Figure 2, where the starting guess links initial positions are shown in Figure 2 a), while, after convergence, the final assembled position is depicted in Figure 2 b). The kinematic analysis is then solved by means of the equations

$$\{\ddot{u}\} = -[\Psi_u]^{-1}[\Psi_v]\{\ddot{v}\} \tag{2}$$

and

$$\{\ddot{u}\} = -[\Psi_u]^{-1}[\Psi_v]\{\ddot{v}\} + \{\gamma\} \tag{3}$$

Where

$$\{\gamma\} = -([\Psi_q] \{\dot{q}\})_q \{\dot{q}\} - 2[\Psi_{qt}] \{\dot{q}\} - \{\Psi_{tt}\} \tag{4}$$

and $[\Psi_u]$ and $[\Psi_v]$ are the jacobian matrices of the vector $\{\Psi(q)\}$, derivative with respect to the coordinates $\{u\}$ and $\{v\}$, respectively.

3.3 Dynamic simulation

According to the method of Lagrangian multipliers, a Differential Algebraic Equations (DAE) system

$$\begin{cases} [M]\{\ddot{q}\} + [\psi_q]^T \{\lambda\} = \{Q\} \\ \{\Psi(q,t)\} = \{0\} \end{cases} \tag{5}$$

can be obtained, where $\{Q\}$ is the generalized force vector, $[M]$ is the system mass matrix and $\{\lambda\}$ is the vector of the $m = 12$ Lagrange multipliers vector. From such system, an Ordinary Differential Equation (ODE) system

$$\begin{cases} [M]\{\ddot{q}\} + [\psi_q]^T \{\lambda\} = \{Q\} \\ [\Psi(q)]\{\ddot{q}\} = \{\gamma\} \end{cases} \tag{6}$$

can be obtained and solved by the classical methods of integrations of ODE systems. However, before integration it is generally convenient reducing the system (4) in a more simple one by eliminating the Lagrange multiplier vector. This can be done in several methods, and the following have been tested for the present problem: coordinate partitioning [2], Udwadia-Kalaba formulation [3], SV Decomposition [4], QR Decomposition [5], Schur Decomposition [6] and the Pennestri's Least-Squares Block Solution [7]. The Baumgarte stabilization method has been also adopted [8].

3.4 Results of simulation

The developed code has been applied to the simulation of a 6 bar linkage in static balance at the initial position. A graphical interface makes the code quite friendly to be used, since the user can select the link lengths, the spring and damper coefficients and the reducing method.

After the application of constant loads on the links, the mechanism showed a damped oscillatory evolution due to the springs and viscous dampers positioned in correspondence of the revolute pairs. With a simulation time of 10 s, the constraint vector norm was of the order of magnitude of 10-10. Simulations can be studied by analyzing directly the numerical data or via graphical interfaces which allow animations or evolutionary diagrams, such as that reported in Figure 3.

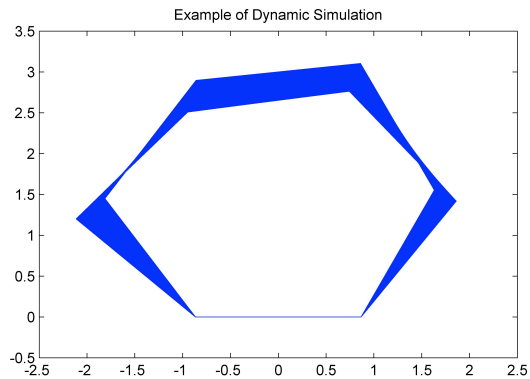


Figure 3. Example of the graphical output, as offered by the program in order to study the simulation results.

4 THE ACTUAL CONSTRUCTION OF PROTOTYPES BY MEANS OF MEMS TECHNOLOGY

The prototypes have been built by means of lift-off methods in order to deposit thick films of metal and by attacking the silicon in order to obtain deep molds. Both surface micromachining and bulk micromachining techniques have been used. In the first case, the mechanism is obtained by depositing or attacking, selectively, the materials directly over the silicon substrate, for thin layers. In the second case, the samples are obtained by attacking deeply the substrate or by depositing material layers thicker than 10 μm .

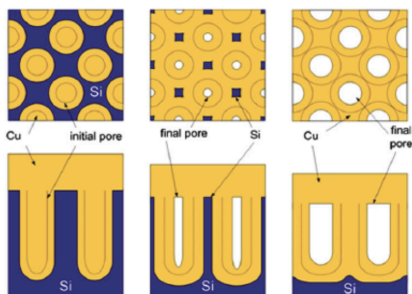


Figure 4: PS-Cu structures which can be obtained by means of the corrosive copper deposition [11]

4.1 Copper prototypes

In the present investigation the first attempt to build a prototype of the mechanism has been based on electro deposition of copper on silicon wafer. The silicon substrate has been previously anodized to make porous its surface before a non-electrochemical process of copper deposition. Two photoresist spinning runs are adopted to reach 16 μm thickness.



Figure 5: One sample of copper prototypes a) and a comparison of it to a 1 Euro cent coin b).

As suggested in [9], porous silicon has been obtained by using silicon as anode and a tungsten cathode in a bath of 3:5:2 solution of hydrofluoric acid (HF) 48%, isopropyl alcohol (IP) and glacial acetic acid (CH_3COOH). According to practice, a continuous current with intensity equal to 20 mA/cm^2 must flow between cathode and anode. Furthermore, corrosive copper deposition can be applied as described in [10], which allows to obtain the structures reported in Figure 4.

The silicon oxide is removed by using a bath of a solution of copper sulfate (CuSO_4) and hydrofluoric acid (HF). In this way, HF improves the current flow, while CuSO_4 allows the deposition of initial copper germs by means of oxide-reduction process.

Finally, copper electro deposition is performed on the samples. Figure 5 shows one prototype sample.

Figure 6 shows the silicon wafer after deposition and photoresist development (a) and the subsequent 9 μm thick copper prototype, obtained with 20 mA/cm^2 current intensity.

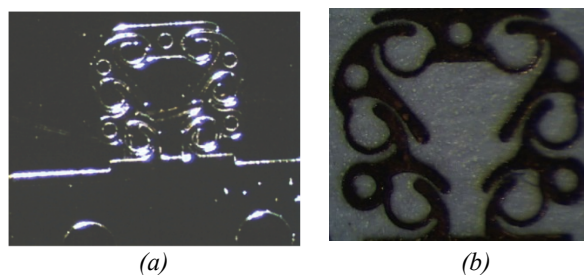


Figure 6: silicon wafer after deposition and photoresist development (a) and the copper prototype (b)

4.2 Silicon prototypes

For the sake of the present investigation, thickness plays a great importance. Therefore, another technique has been analyzed in order to achieve a thicker compliant mechanism, up to 50 μm .

With reference to Figure 7 a), a 1 μm layer of aluminum is firstly deposited on a 50 μm thick silicon wafer by sputtering aluminum in a chamber with 100 sccm of Argon, at a pressure of $1.9 \cdot 10^{-2}$ mbar. The photoresist is overlaid on aluminum (see Figure 7 b) and the mask is positioned over the wafer. The UV exposure, as represented in Figure 7 c, transfers the mask geometry on the sample by PR developing, as represented in Figure 7 d). Then, the unprotected Aluminum layer is etched, at a rate of 10 $\text{\AA}/\text{s}$, by a solution of phosphoric acid (80 ml), nitric acid (5 ml) and deionized (DI) water (10 ml) and the geometry is transferred on aluminum as in Figure 7 e). Finally, RIE (Reactive Ion Etching) is applied on a 50 μm wafer by means of a $\text{SF}_6 + \text{O}_2$ (50sccm + 2sccm) gas mixture at a pressure of 80 mTorr with a power of 250W for 90 minutes. The upper layer is then removed by a final etching for the aluminum.

Some examples of silicon prototypes are shown in Figures 8 and 9.

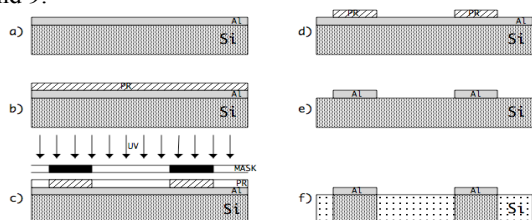


Figure 7. The process phases adopted in the present investigation.

5 CONCLUSIONS

A code for the dynamic simulation of a 3 D.O.F. MEMS has been developed in MatLab programming language. The program was able to simulate the motion of the mechanism under several dynamic conditions. For example, an oscillatory motion was simulated by applying, at the initial time, a concentrated load on the undeformed structure, assuming certain values of the viscous damping coefficients (they take into account both the material damping and the viscous friction coefficient).



Figure 8: silicon prototype with 4 actuating cables.

The simulations have shown good accordance with the FEA models (at stationary state) and with the experimental motion of a major scaled prototype. However, such results could not be considered as conclusive, because the one-to-one scale prototypes may behave differently from the scaled ones. Hence, some real size (3 mm \times 3mm) prototypes of the new MEMS have been built for the future investigation. This paper also describes how such prototypes were developed, by using some typical processes: copper electro deposition and RIE on silicon

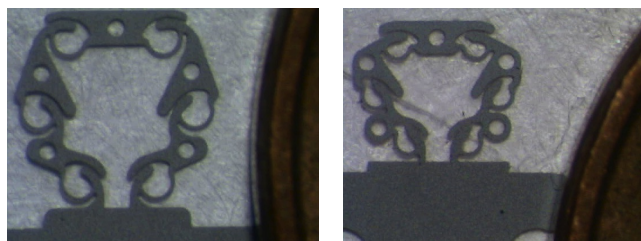


Figure 9: two samples of silicon prototypes.

REFERENCES

- [1] Belfiore N.P., Scaccia M., Ianniello F., Presta M., Selective compliance hinge, World Intellectual Property Organization, WO/2009/034551, Int. Appl. No. PCT/IB2008/053697, Publ. Date March, 19th, 2009.
- [2] Wehage RA, Haug EJ. ASME Journal of Mechanical Design 1982; 134:247–255.
- [3] Udwadia FE, Kalaba RE. Analytical Dynamics a New Approach. Cambridge University Press: Cambridge, 1996.
- [4] Mani NK, Haug EJ, Atkinson KE. ASME Journal of Mechanisms, Transmissions, and Automation in Design 1985; 107:82–87.
- [5] Kim SS, Vanderploeg MJ. ASME Journal of Mechanisms, Transmissions, and Automation in Design 1986; 108:176–182.
- [6] Pennestri E, Valentini PP. Coordinate reduction strategies in multibody dynamics: a review. Proceedings of the Conference on Multibody System Dynamics, London, 2007.
- [7] Pennestri E, Vita L, de Falco D. Journal of Aerospace Engineering 2008; 22:365–372.
- [8] Vlasenko D, Kasper R. Multibody System Dynamics 2009; 22:297–315.
- [9] V. Lehmann, Electrochemistry of Silicon: Instrumentation, Science, Materials and Applications. Ed. Wiley-VCH, 2002
- [10] H. Bandarenka, M. Balucani, R. Crescenzi, A. Ferrari. Superlattices and Microstructures 44 (2008) 583-587